Journal of Power Sources 196 (2011) 894–898

Contents lists available at ScienceDirect

Journal of Power Sources

journal homepage: www.elsevier.com/locate/jpowsour

Enhanced conductivity and stability of composite membranes based on poly (2,5-benzimidazole) and zirconium oxide nanoparticles for fuel cells

Haitao Zheng*, Mkhulu Mathe

Materials Science and Manufacturing, Council for Scientific and Industrial Research (CSIR), Pretoria, South Africa

ARTICLE INFO

Article history:
Received 20 January 2010
Received in revised form 30 August 2010
Accepted 16 September 2010

Keywords:
Poly (2,5-benzimidazole)
ZrO_2
Nanoparticles
Membrane
Fuel cells

ABSTRACT

Poly (2,5-benzimidazole) (ABPBI) and zirconium oxide (ZrO_2) nanoparticles composite membranes were synthesized. These membranes can be fabricated into tough, dense membranes by blending Poly (2,5-benzimidazole) (ABPBI) with zirconium oxide (ZrO_2) nanoparticles, which were characterized by using FTIR, XRD, SEM, TGA, DSC and tensile test. These composite membranes showed increased conductivity compared with original ABPBI membrane. Maximum proton conductivity at 100 °C was found to be 0.069 S cm^{-1} on 10% ZrO_2 incorporated ABPBI composite membrane, almost four times as high as the 0.018 S cm^{-1} obtained in the case of the ABPBI membrane. The conductivity was 0.0325 S cm^{-1} at 180 °C in dry condition for ABPBI with 10% ZrO_2 nanoparticles composite membrane, higher than the conductivity 0.011 S cm^{-1} of the ABPBI membrane at same condition. Furthermore, the composite membranes were shown to have high thermal and mechanical stability. These results suggest that ABPBI/ZrO_2 composite membranes may be a promising polymer electrolyte for fuel cells at medium or high temperature, due to their strong physical properties.

1. Introduction

In recent years, research activities in polymer electrolyte membrane fuel cells (PEMFCs) have grown with a sign of stepping. PEMFC operated at high temperature, in particular, continues to generate interest in regards to the prevention of catalyst poisoning of CO, improved electrode reaction kinetics, and enhanced system efficiency [1,2]. In spite of these advantages, the actual use of high temperature PEMFCs for production of energy is still quite limited, with one of the major challenges as the design of stable proton conducting membrane that provides good performance above 100 °C. Perfluorosulphonic acid membranes (e.g., DuPont's Nafion) have been extensively investigated as polymer electrolyte for fuel cells which requires water for proton conduction [3,4]. Therefore, the operating temperature is typically limited to below 100 °C. Much research efforts have been devoted to the study of proton conducting membranes at temperatures above 100 °C. Savinell et al. [5,6] first developed polybenzimidazole (PBI) that can be used as a polymer electrolyte at 200 °C after doping with strong acids such as phosphoric acid (H_3PO_4) or sulphuric acid (H_2SO_4). The PBI membrane has high conductivity and high thermal stability [7]. Some research groups have focused their interests on another benzimidazole polymer poly (2,5-benzimidazole) (ABPBI) with comparable thermal and conductance properties to that of PBI [7–9]. Poly (2,5-benzimidazole) (ABPBI) though can be synthesized by a simpler route than PBI. ABPBI membrane doped phosphoric acid has been used successful as a good electrolyte for H_2/O_2 fuel cells at temperatures up to 180 °C [10,11]. A PEMFC operating at 210 °C can tolerate about 1.0 vol.% of CO in the H_2 feed without any performance loss [9]. However, ABPBI membranes also needs improvement since they could be benefit from higher conductivity and have been shown to suffer from phosphoric acid leaking upon extended use under harsh working conditions.

Zirconium phosphate is an inorganic proton conductor, which could enhance proton conduction as a composition of membrane for fuel cells. Various aspects of research done recently on the development of zirconium phosphate composite membranes for PEM fuel cell applications were surveyed by Savadogo [12]. Grot and Rajendran [13] prepared a nanocomposite of Nafion with zirconium hydrogen phosphate (ZHP) which was precipitated in Nafion matrix by in situ reaction of $ZrOCl_2$ and H_3PO_4 at 80 °C. Kim et al. [14] prepared zirconium sulphophenyl phosphate (ZrSPP) by the reaction of Zr^{4+} ion and *m*-sulphophenyl phosphonic (SPP) acid in the presence of HF in order to increase the proton conductivity of the inorganic filler. Kim et al. [15] synthesized zirconium pyrophosphate (ZPP)/Poly (2,5-benzimidazole) (ABPBI) composite; they reported that the incorporation of 10–20%/ZPP into the membrane improved the thermal and dimensional stabilities of the membrane. These methods revealed some limitations such as a complex preparing procedure and big zirconium phosphate particles. Zirconium oxide

* Corresponding author. Tel.: +27 12 841 2389; fax: +27 12 841 2135.
E-mail addresses: hzheng@csir.co.za, zhenght08@gmail.com (H. Zheng).

0378-7753/$ – see front matter.
doi:10.1016/j.jpowsour.2010.09.028

(ZrO_2) is used in oxygen sensors and fuel cell membranes because it has an ability to allow oxygen ions to move freely through the crystal structure at high temperatures [16]. Carriere et al. [17] has shown that crystalline nanometric zirconium oxide (ZrO_2) is a good substrate for organic grafting via the zirconium phosphate bond. Vaivars et al. [18] prepared inorganic proton conducting membranes for DMFCs by impregnating an inorganic porous substrate with ZrO_2 particles and by subsequent phosphorization. However, ABPBI composite membrane using ZrO_2 nanoparticles as an assistant have not been reported in the literature to date.

In this work, a different method is put forward for the beneficial effects of the ZrO_2 nanoparticles on function of ABPBI membrane as an electrolyte for high temperature PEMFC.

2. Experimental

2.1. Materials

3,4-Diaminobenzoic acid (DABA) 97% was used without further purification. 99% methanesulphonic acid (MSA), Polyphosphoric acid (PPA) 85%, white mineral oil and phosphoric acid (85%) were purchased from Aldrich. Zirconium oxide (ZrO_2) nanoparticles were purchased from Degussa (average particles size 20–40 nm).

2.2. Polymer synthesis

ABPBI polymer was synthesized in PPA from the DABA monomer at 180 °C for 5 h [19] as presented in the scheme below.

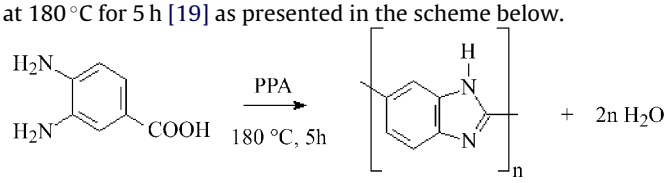

The procedure followed was: 13.0 g of 3.4-diaminobenzoic acid and 100 ml of white mineral oil were added in a 3-neck glass flask equipped with a mechanical stirrer under a nitrogen atmosphere. The mixture was stirred well and 60 g of polyphosphoric acid was added while stirring. The mixture was then heated to 160 °C, and held at this temperature for 2 h with continuous stirring, forming gray-black materials. After the mixture cooled down, the product was removed from mixture by filtration. The product was neutralized with sodium carbonate, filtered, and washed with de-ion water and then acetone. Then it was dried in a vacuum oven at 110 °C over night.

2.3. Preparation of ABPBI membranes and ABPBI/ZrO_2 membranes and H_3PO_4 doping

The ABPBI membranes were prepared by evaporation of MSA solution [20]. The ABPBI polymer was dissolved in MSA at 130 °C to make a 4% solution. The viscous solution was then casted onto flat bottom glass plates and the solvent was removed by heating the plates in a ventilated oven at 200 °C until volatility ceased. Then, the plates were cooled down to 100 °C and hot water poured over it to peel off the membranes. Subsequently the membranes were dried in a vacuum oven at 110 °C over night. The thickness of membranes were 0.05–0.06 mm. The preparation of the ABPBI/ZrO_2 nanoparticles composition membrane was done by adding ZrO_2 nanoparticles to the MSA solution. This suspension was stirred at 70 °C for 3 h and then the ABPBI solution was added while stirring for 4 h. And ABPBI/ZrO_2 composition membranes were prepared by the process similar to that of ABPBI membrane. The amount of ZrO_2 nanoparticles used in these reactions respectively was 5%, 10% and 15% of ABPBI polymer. The names of these composites were also noted as ABPBIZ5, ABPBIZ10 and ABPBIZ15.

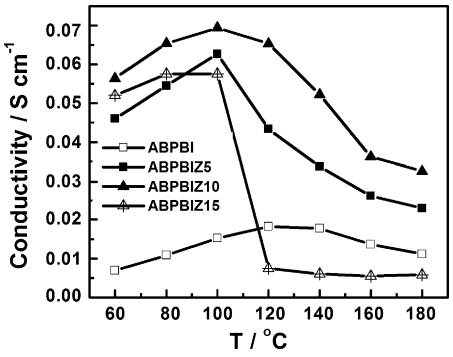

Fig. 1. Proton conductivities of ABPBI, ABPBIZ10 and ABPBIZ15 membrane doped with H_3PO_4 as a function of temperature.

The dried ABPBI and ABPBI/ZrO_2 nanoparticles composition membrane were immersed in 85% H_3PO_4/H_2O (70:30 by volume) for 3 days at 70 °C.

2.4. Characterization

AC conductivity measurements as a function of temperature were made in air using a Hioki 3560 AC milliohm meter (HiTester). The area of electrode was 4 cm^2. The membrane was sandwiched between carbons electrode and packed in a sealed cell. The membrane in a test cell for conductivity was operated with a preceding hot-pressing step, with 20 kg cm^{-2} at 110 °C for 2 min. The proton conductivity of membrane was calculated using the relation $\sigma = d/RS$, where d, R and S are the thickness, resistance and face area of the membranes, respectively. The contact resistance between the cell components have been lumped with the membrane resistance. However, it was quite low compared with the membrane resistance.

Thermal gravimetric analysis (TGA) was done using Thermal Analyzer STA 1500 (CCI-3, Rheometric Scientific) at air with 10 °C min^{-1}.

Differential scanning calorimetry (DSC) measurements were done by using DSC Q2000 under nitrogen atmosphere heating from room temperature up to 400 °C at a rate of 20 °C min^{-1}.

The membrane morphology was studied with a Scanning Electron Microscope (SEM, Hitachi X650). The samples were Au-sputtered under vacuum before the SEM examination.

Fourier Transform Infrared (FTIR) spectra were recorded on Perkin Elmer Paragon 1000 Fourier transform spectrometer.

The effect of a constant stress on the different membranes was evaluated by tensile testing on H10KT tensile test machine (Tinius olsen). The membranes were cut into samples with a length and width of 5 and 1.0 cm. Stress–strain cures were generated using a strain rate of 0.5 mm min^{-1} and an initial static force of 50 N at room temperature.

3. Results and discussion

3.1. Conductivity

Some reports [21,15] showed optimized inorganic material added into polymer were below 20%. On this case of ABPBI polymer, we have studied 5–15% ZrO_2 added ABPBI membranes. Fig. 1 shows the proton conductivities of ABPBI membrane and ABPBI/ZrO_2 composite membranes doped with H_3PO_4 as a function of temperature. The proton conductivity of ABPBI/ZrO_2 doped with H_3PO_4 composite membrane were increased with the introduction of ZrO_2, A maximum conductivity was founded to be 0.069 S cm^{-1} on the ABPBIZ10 composite membrane at 100 °C. Maximum conductiv-

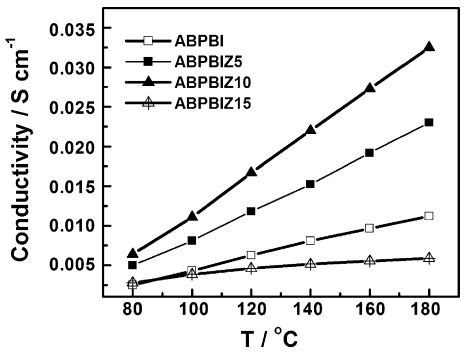

Fig. 2. Proton conductivities of ABPBI, ABPBIZ10 and ABPBIZ15 membrane doped with H_3PO_4 in dry condition.

ity was 0.018 S cm^{-1} at 120 °C for the ABPBI membrane, which is three times much lower than the ABPBIZ10 composite membrane. As presented in Fig. 1, the order of maximum conductivity is ABPBIZ10 > ABPBIZ5 > ABPBIZ15 > ABPBI membrane. Then with increased temperature, the proton conductivity of the ABPBI membrane and the ABPBI/ZrO_2 composite membranes were dropped. For this case of ABPBI-ZrO_2 membranes, the conductivity failure above a certain temperature could be associated with different expansion of the filler and the polymer as a consequence of changes in temperature. It is likely that humidification still plays a vital role in conductivity although H_3PO_4 is considered a proton donor for conductance at high temperature. This is supposed to also lower relative humidity leading to less conductive species due to the losing of phosphoric acid-water equilibriums [22].

To further eliminate the effect of absorbed humidity of the membrane under air condition, the cell was heated at 180 °C until it stabilized and the measurements of conductivity were recorded while cooling as presented in Fig. 2. ABPBIZ10 composite membranes still maintained excellent conductivity compared with ABPBIZ5, ABPBIZ15 and ABPBI membranes in dry condition. A maximum conductivity of 0.0325 S cm^{-1} of ABPBIZ10 composite membrane was achieved at 180 °C in a dry condition, almost three times higher than that of the case of ABPBI membrane (0.011 S cm^{-1}). This value is similar to the conductivity of ABPBI-PMo_{12} membrane reported by Gómez-Romero et al. [9] (0.03 S cm^{-1} at 185 °C), slightly lower than that of 0.04 S cm^{-1} at 180 °C (5%RH) for ABPBI 2.7 phosphoric reported by Kim et al. [7]. However, the conductivity of ABPBIZ10 composite membrane in this work is much lower than that of ABPBI-$Zr(HPO_4)_2$ composite membrane [15] due to the different manufacturing process and casting method of the membrane.

3.2. Morphology

Fig. 3 shows the SEM morphology of surface and a cross-section of the ABPBIZ10 composite membrane and ABPBI membrane. Fig. 3a shows the ABPBI membrane has compact distribution without holes. Fig. 3b depicts the effect of the addition of the ZrO_2 nanoparticles filler to the ABPBI matrix without pores. Compared with the ABPBI membrane, the ABPBIZ10 composite membrane displays a fairly evident change in the ionomer morphology (see Fig. 3c and d). However, Fig. 3d shows the absence of phase separation as observed in the case of the ABPBZ10 composite membrane, suggesting that the synthesized composite membranes were homogeneous in nature and hence formed dense membranes.

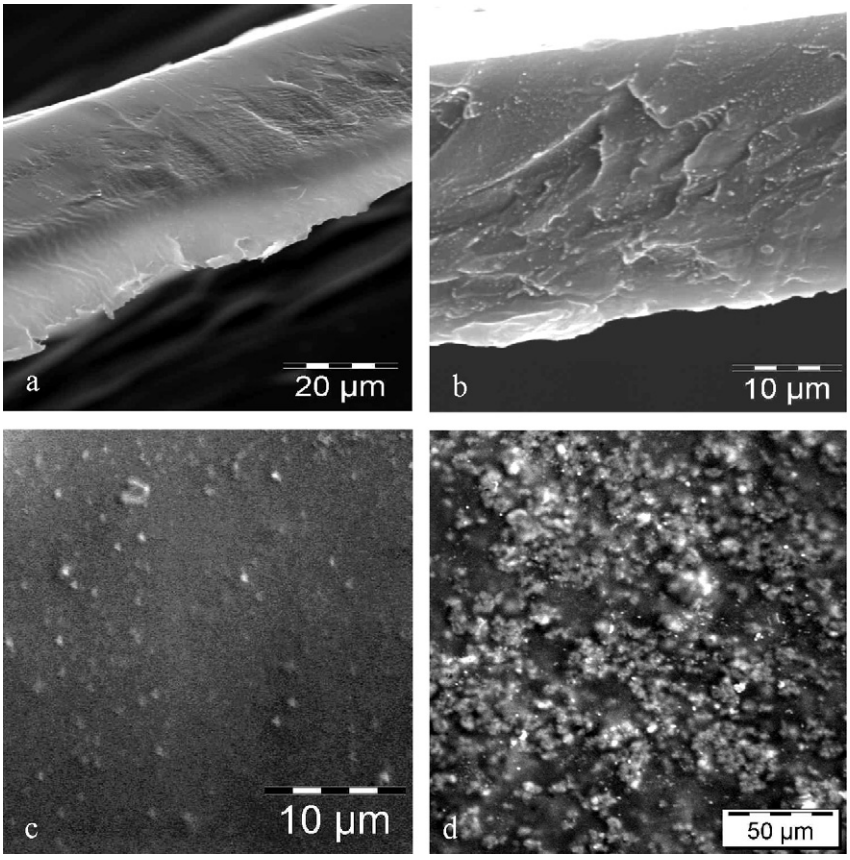

Fig. 3. SEM image of cross-section (a) and surface (c) of ABPBI membrane; cross-section (b) and surface (d) of ABPBIZ10composite membrane.

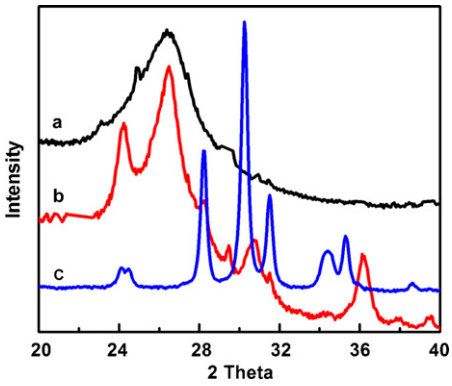

Fig. 4. XRD patters of ABPBI (a), ABPBIZ10 (b) and ZrO_2 nanoparticles (c).

3.3. XRD analysis

Fig. 4 shows the XRD patterns of the ABPBIZ10 composite membrane and ABPBI membrane without H_3PO_4. The ABPBI membrane showed a broad peak at around 26°. This peak is ascribed to a *d* spacing of 3.3 Å between ABPBI chains [23]. For ABPBIZ10 composite membrane, sharper peaks around 24.2°, 29.5°, 30.8°, 31.5°, and 36.2° were observed, in addition to the sharper peak 26.5° from ABPBI. These observed peaks are attributed to ZrO_2 in the composite membrane (Fig. 4c). We can see from Fig. 4, the peak at 26° in ABPBIZ10 composite is more resolved than that of the ABPBI membrane, suggesting that crystallinity of the ABPBI structure was increased by adding ZrO_2 nanoparticles.

3.4. FT-IR spectra

The FT-IR spectrum of the ABPBI membrane and the ABPBIZ10 membrane doped/undoped with H_3PO_4 are given in Fig. 5 The C=N and C=C stretching bands for benzimidazole at 1620 and 1445 on ABPBI membrane undoped/doped with H_3PO_4 [8]. As seen in Fig. 5, the spectrums of all samples, in the range 3600–2000 cm^{-1}, results from N^+–H stretching vibration [24–25]. P–O stretching band was observed at 1000–1013 cm^{-1} due to N^+–H stretching vibrations in the acid doped ABPBI membrane and ABPBIZ10 composite membranes [26]. It is shown on Fig. 4c that broad bands at 450, 716, 812, and 3718 cm^{-1} related to the ZrO_2 phase [27–28]. After doped with H_3PO_4, on ABPBIZ10 membrane, the characteristic peak 1720–1750 cm^{-1} and 3785 are due to P–OH and ZrOH groups, respectively [29–30].

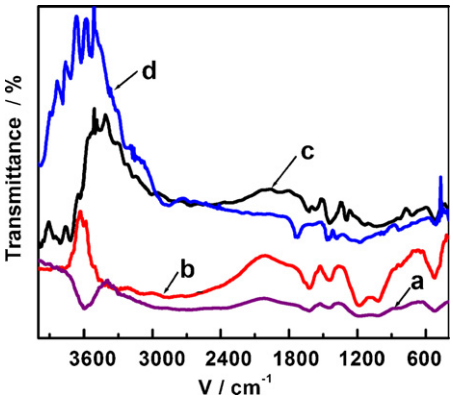

Fig. 5. FT-IR spectra of ABPBI, ABPBIZ10 in the absence/presence of H_3PO_4. ((a) ABPBI; (b) ABPBI-doped H_3PO_4; (c) ABPBIZ10; (d) ABPBIZ10-doped H_3PO_4.)

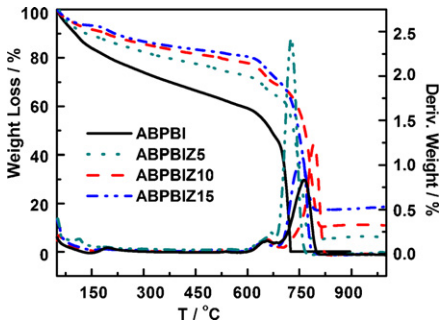

Fig. 6. TGA and DTA of ABPBI, ABPBIZ5, ABPBIZ10 and ABPBIZ15 membrane doped with H_3PO_4.

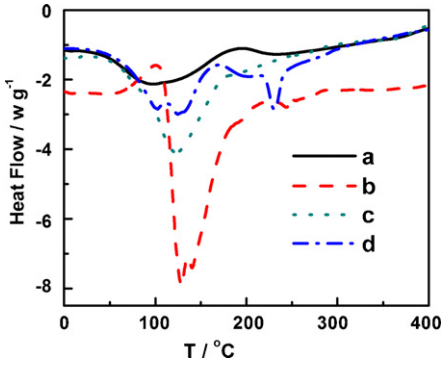

Fig. 7. DSC of ABPBI and ABPBIZ10 membranes doped with H_3PO_4. ((a) ABPBI; (b) ABPBI-doped H_3PO_4; (c) ABPBIZ10; (d) ABPBIZ10-doped H_3PO_4.)

3.5. Thermal analysis

The thermal stability was studied by TGA and DTA on ABPBI membrane and ABPBI/ZrO_2 doped H_3PO_4 composite membranes. As shown on Fig. 6, most water is lost below 100 °C and decrease the weight at around 200 °C may be caused by condensation reaction of phosphoric group with the dehydration. The initial temperature on 20% weigh loss of the ABPBIZ5, ABPBIZ10 and ABPBIZ15 membrane were 370, 525 and 620 °C, respectively. And the maximum exothermic peak of, ABPBIZ5, ABPBIZ10 and ABPBIZ15 membrane were 724, 760 and 790 °C. While it was 200 °C for decomposition temperature (20% weigh loss) and was 765 °C for the maximum exothermic peak of the ABPBI membrane. These results indicated that ABPBI/ZrO_2 composite membranes have higher thermal stability than the pure ABPBI membrane. The residual mass should be identical with that of ZrO_2 included in ABPBI/ZrO_2 composite membranes. These residual masses are 5.3, 10.2 and 17.2 wt.% for the ABPBIZ10 and ABPBIZ15 composite membrane, respectively. Obviously, this value for ABPBIZ15 is slight higher than the amount of 15 wt.% ZrO_2, added in the beginning of polymerization. This could indicate that probably some ZrO_2 nanoparticles are able to aggregate within the polymeric matrix so as to form filler rich pathways.

The DSC of the ABPBI membranes and ABPBIZ10 composite membranes is presented in Fig. 7. Endotherms shown in Table 1

Table 1
Endotherm values (*T*) of ABPBI and ABPBIZ10 undoped and doped with H_3PO_4 membranes calculated from DSC.

Membrane	*T* (°C)
ABPBI	104
ABPBIZ10	120
ABPBI-doping H_3PO_4	100, 125, 230
ABPBIZ10-doping H_3PO_4	128, 140, 244

Table 2
The tensile properties of ABPBI, ABPBIZ5, ABPBIZ10 and ABPBI Z15 membranes.

Membranes	ABPBI	ABPBIZ5	ABPBIZ10	ABPBIZ15
Yield stress (MPa)	19.1	69.0	87.5	42.4
Young's modulus (GPa)	2.4	3.2	4.8	8.1
Elongation at break (%)	19.2	16.6	4.6	4.5

indicate the existence of single endotherm for both membranes without doping H_3PO_4, attributable to the loss of absorbed water of ABPBI [30,31]. In the case of ABPBI doped with H_3PO_4 membranes, there are three endotherms at 100, 125 and 230 °C, which can all be ascribed to the loss of the surface absorbed water of ABPBI membrane, of the bound water of the ABPBI matrix and condensation of the PO_4 groups. The ABPBIZ10 doped H_3PO_4 composite membranes indicate three endotherms at 128, 140 and 244 °C [32–34]. These valves are slightly higher than those of the ABPBI membrane, an indication that the ABPBIZ10 composite membrane have a stronger bound force with water than that of the ABPBI membrane. These results further indicated that the ABPBIZ10 composite membrane have higher thermal stability than the ABPBI membrane.

3.6. Mechanical characterizes

Table 2 summarizes the results obtained during the mechanical characterization of the ABPBI/ZrO_2 composite membranes. Yield stress is used as an indication of the onset of plastic deformation and Young's modulus as an indication of stiffness [35]. From Table 2, the yield stress and Young's modulus on ABPBI/ZrO_2 composite membranes are presented as being much higher than that of ABPBI membrane. The yield stress of ABPBIZ10 membranes was 87.5 MPa which is about four times more than that of 19.1 MPa for the ABPBI membrane, the yield stress that was attained on the ABPBIZ5 membrane was 69.0 MPa, which is more than three times that of the ABPBI membranes. On the ABPBIZ15 composite membrane, doubled the yield stress of the ABPBI membrane. The Young's modulus on the ABPBI/ZrO_2 composite membranes was increased by the weight of ZrO_2 added in membrane. For the ABPBIZ10 membranes, the Young's modulus was 4.8 GPa, whereas it was 2.38 GPa in the case of ABPBI membranes. The Young's modulus obtained by the ABPBI casted at a high temperature and low temperature is about 1.19 and 0.290 GPa [36], respectively and are smaller than these obtained in this work. A possible reason for those differences are through variations in the manufacturing process, casting process, and the inorganic ZrO_2 nanoparticles added. These results show that the incorporation of ZrO_2 into the ABPBI increased the anti-deformation capability and stiffness of the composites. Reduced elongation exhibited on the ABPBI/ZrO_2 composite membranes might be due to poor nonexistent adhesion between the rigid particulate ZrO_2 filler and the polymeric matrix. The stress is not transmitted to the filler by the polymer chains and, thus, the reinforcement effect is eliminated in the ABPBI/ZrO_2 composite membranes [37].

Furthermore, we also examined the stability of ABPBI and ABPBIZ10 membranes in 85% phosphoric acid solution. We found that the ABPBI membrane starting to dissolve after 3 h and 50% dissolved for 24 h when it was immersed in 85% phosphoric acid solution. However, ABPBIZ10 membrane still maintained its mechanical integrality when it was immersed in 85% phosphoric acid solution for 24 h, indicating that ZrO_2 nanoparticles increased the dimensional stability [15].

4. Conclusions

ABPBI/ZrO_2 composite membranes have been synthesized based on ABPBI matrix ZrO_2 nanoparticles. These ABPBI/ZrO_2composite membranes have shown a considerable increase in conductivity, with enhanced thermal stability and mechanical anti-deformation, compared with the original ABPBI membrane. For conductivity, 0.069 S cm^{-1} of maximum proton conductivity was found on the ABPBIZ10 doped composite membrane at 100 °C, almost four times as high as that of original ABPBI membrane. Maximum conductivity of 0.0325 S cm^{-1} at 180 °C was attained with ABPBIZ10 composite membrane in dry conditions that was higher than the conductivity 0.011 S cm^{-1} obtained from original ABPBI membrane at the same conditions. The incorporation of 5–15 wt.% ZrO_2 nanoparticles into the ABPBI membrane improved the thermal and mechanical stabilities of the membrane. Furthermore, the ABPBIZ10 composite membrane immersed in 85% phosphoric acid solution for 24 h whilst maintained its mechanical integrity.

References

[1] K. Sopian, W. Ramli, W. Daud, Renew. Energy 31 (2006) 719–724.
[2] J.L. Zhang, Z. Xie, J.J. Zhang, Y.H. Tang, C.J. Song, T. Navessin, Z.Q. Shi, D.T. Song, H.J. Wang, D.P. Wilkinson, Z.S. Liu, S. Holdcroft, J. Power Sources 160 (2006) 872–891.
[3] J.J. Grodzinski, Polym. Adv. Technol. 18 (2007) 785–868.
[4] P. Choi, N.H. Jalani, T.M. Thampan, R. Datta, J. Polym. Sci. B 44 (2006) 2183–2200.
[5] J.S. Wainright, J.T. Wang, R.F. Savinell, M.H. Litt, J. Electrochem. Soc. 142 (1995) L121–L123.
[6] D. Weng, J.S. Wainright, U. Landau, R.F. Savinell, J. Electrochem. Soc. 143 (1996) 1260–1263.
[7] H.J. Kim, S.Y. Cho, S.J. An, Y.C. Eun, J.Y. Kim, H.K. Yoon, H.H. Kweon, K.H. Yew, Macromol. Rapid Commun. 25 (2004) 894–897.
[8] J.A. Asensio, S. Borrós, P. Gómez-Romero, J. Electrochem. Soc. 151 (2004) A304–A310.
[9] J.A. Asensio, S. Borrós, R. Ruiz, P. Gómez-Romero, Eletrochem. Commun. 5 (2003) 967–972.
[10] P. Krishnan, J.S. Park, C.S. Kim, J. Power Sources 159 (2006) 817–823.
[11] J.A. Asensio, S. Borrós, R. Ruiz, P. Gómez-Romero, Proceedings of the 203th Meeting of the Electrochemical Society, Paris, 2003.
[12] O. Savadogo, J. Power Sources 127 (2004) 135–161.
[13] W.G. Grot, G. Rajendran, US Patent 5,919,583 (1999).
[14] Y.T. Kim, M.K. Song, K.H. Kim, S.B. Park, S.K. Min, H.W. Rhee, Electrochim. Acta 50 (2004) 645–648.
[15] T.H. Kim, T.W. Lim, Y.S. Park, K. Shin, J.C. Lee, Macromol. Chem. Phys. 208 (2007) 2293–2302.
[16] A.H. Heuer, L.W. Hobbs (Eds.), Science and Technology of Zirconia, Adv. Ceram., vol. 3, ACerS, Columbus, OH, 1981, p. 475.
[17] D. Carriere, M. Moreau, K. Lhalil, P. Barboux, J.P. Boilot, Solid State Ionics 162 (2003) 185–190.
[18] G. Vaivars, T. Mokrani, N. Hendricks, V. Linkov, Solid State Electrochem. 8 (2004) 882–885.
[19] N. George, J. Milford, V. Waynesboro, US Patent 4,460,763 (1984).
[20] T.E. Helminiak, C.L. Benner, F.E. Anold, G. Husman, US Patent 4,377,546 (1983).
[21] M.L. Ponce, L. Prado, B. Ruffmann, K. Richau, R. Mohr, S.P. Nunes, J. Membr. Sci. 217 (2003) 5–15.
[22] Y.L. Ma, J.S. Wainright, M.H. Litt, R.F. Savinell, J. Electrochem. Soc. 151 (2004) A8–A16.
[23] A. Wereta Jr., M.T. Gehatia, Polym. Eng. Sci. 18 (1978) 204–206.
[24] R. Bouchet, E. Siebert, Solid State Ionics 118 (1999) 287–299.
[25] A.M. Bellocq, C. Perchard, A. Novak, M.L. Josien, J. Chim. Phys. 62 (1965) 1334–1342.
[26] P. Colomban, A. Novak, J. Mol. Struct. 198 (1989) 277–280.
[27] M. Salavati-Niasari, M. Dadkhah, F. Davar, Polyhedron 28 (2009) 3005–3009.
[28] H.G. Bernal, L.C. Caero, E. Finocchio, G. Busc, Appl. Catal. A: Gen. 369 (2009) 27–35.
[29] G.A.H. Mekhemer, Colloids Surf. A: Physicochem. Eng. Aspects 141 (1998) 227–235.
[30] A.A. Tsyganenko, V.N. Filimonov, J. Mol. Struct. 19 (1973) 579–589.
[31] N.W. Brooks, R.A. Duckett, J. Rose, I.M. Ward, J. Clements Polym. 34 (1993) 4038–4042.
[32] O. Acar, U. Sen, A. Bozkurt, A. Ata, Int. J. Hydrogen Energy 34 (2009) 2724–2730.
[33] A. Carollo, E. Quartarone, C. Tomasi, P. Mustarelli, F. Belotti, A. Magistris, L. Garlaschelli, P.P. Righetti, J. Power Sources 160 (2006) 175–180.
[34] S.R. Samms, S. Wasmus, R.F. Savinell, J. Electrochem. Soc. 143 (1996) 1225–1232.
[35] S. Kundu, L.C. Simon, M. Fowler, S. Grot, Polymer 46 (2005) 11707–11715.
[36] E.A. Franceschini, H.R. Corti, J. Power Sources 188 (2009) 379–386.
[37] A. Eisenberg, J. Kim, Introduction to Ionomers, Wiley, New York, 1998.